

doi:10.15199/48.2022.05.26

Power quality enhancement in wind turbine based DFIG using fuzzy control and neural-RIP for harmonic mitigation

Abstract. Harmonic issue in the wind power plant is a concerning problem for both consumers and producers as that it affects the power quality of the distribution systems. This paper presents an improved control strategy for harmonic current compensation in wind turbine-based DFIG connected to the grid, using RIP-ADALINE for harmonic currents detection. A vector control-based fuzzy logic controller is applied to improve the active and reactive power flow. The active filtering is achieved using the grid side converter of the DFIG. The studied system has been simulated using MATLAB/SIMULINK platform. The results obtained show the effectiveness of the control strategies applied to the system. Therefore the power quality in terms of grid current waveform, total harmonic distortion (THD) factor, frequency spectrum, and system power factor is improved within permissible standard values as defined by IEEE-519

Streszczenie. Zagadnienia harmoniczne w elektrowni wiatrowej stanowią problem zarówno dla odbiorców, jak i producentów, ponieważ wpływają na jakość energii elektrycznej w systemach dystrybucyjnych. W artykule przedstawiono udoskonaloną strategię sterowania kompensacją harmonicznym prądu w elektrowni wiatrowej DFIG podłączonej do sieci, wykorzystującą RIIP-ADALINE do wykrywania harmonicznym prądu. Do poprawy przepływu mocy czynnej i biernej zastosowano sterownik wektorowy oparty na logice rozmytej. Filtracja czynna jest realizowana przy użyciu przekształtnika DFIG podłączonego do sieci. Badany system jest symulowany przy użyciu platformy MATLAB/SIMULINK. Uzyskane wyniki wskazują na skuteczność zastosowanych strategii sterowania, dlatego jakość energii elektrycznej w zakresie kształtu przebiegu prądu sieciowego, współczynnika całkowitych zniekształceń harmonicznym (THD), widma częstotliwości oraz współczynnika mocy systemu została poprawiona w zakresie dopuszczalnych wartości standardowych określonych przez IEEE-519. (Poprawa jakości energii w DFIG opartym na turbinie wiatrowej przy użyciu sterowania rozmytego i neural-RIP w celu łagodzenia harmonicznym)

Keywords: wind turbine-power quality-harmonic-Adaline.

Słowa kluczowe: turbina wiatrowa-jakość energii-harmoniczna-adaline.

Introduction

Nowadays, the wind energy is considered as promising renewable energy due to its rapid development in recent years and its advantages such as low pollution, comparatively low capital cost involved [1,2,3]. Wind turbines based doubly-fed induction generator DFIG are commonly used and preferable over the other types of machines for the benefits that offer such as its ability to supply power both at lagging and leading power factor [4].

The stator of this machine is linked directly to utility grid while its rotor is connected throughout back-to-back converters which are presented in rectifier and inverter that ensure the conversion of the full rated output of the machine to power that is compatible with the grid power. It should be highlighted that the using of power electronic devices lead to the harmonic currents emissions, they affects directly the quality standards of the supplied voltage.[5]In order to reduce the impact of harmonic currents in the electric system at the point of common coupling ,passive filters were initially proposed for their simple structure and easy design ,despite of their advantages, they also present some disadvantages such as parallel resonance with the system impedance at a frequency below the tuned frequency, which causes current magnification; therefore, it would be less efficient in harmonic reduction .To avoid the drawbacks of passive filters , modern active harmonic filters (APFs) were proposed [6] . An active filter consists of three parts: identification, modulation, and inverter. The performance of the active filter is mostly determined by the approach used to calculate the reference current and the control mechanism used to inject the required compensating current into the line [6,7].

The similar structure of the shunt active filter to the converters of the DFIG make it possible to use them in harmonic mitigation therefore various studies have studied the employment of the converters of DFIG as a shunt active filter. In [10,11], the authors have studied the use of the

rotor side converter (RSC) to achieve the compensation of reactive power in addition to the active filtering of harmonics grid currents, a similar study has been achieved in [12]. The active filtering strategy employing RSC control might lead to an unsatisfactory operation resulting in a reduction in its usable life due to that the injected current harmonics in DFIG, and the electric machine is not suited for it, which increases losses. Recently studies focus on compensating harmonic currents based on the use of the grid side converter (GSC) as an active filter. In [13] a GA optimization method was applied to extract the MPPT when the wind speed changes, the GSC is used as SAPF. The d-q synchronous reference frame axis is implemented for the reference extracting harmonic currents in case of using nonlinear load. A hysteresis current controller was used to generate the pulses of the converters.

In [14] the instantaneous power PQ theory was applied to calculate the harmonic currents references. In [15] the active filtering was added to the GSC and the synchronous reference frame (SRF) method was used to determine the harmonic current. The system studied was achieved using MATLAB /Simulink and validated experimentally for the operation of DFIG. In [16] The active filtering is carried out via an algorithm that employs the conservative power theory (CPT) mathematical formulation used in the electrical current control loop on the grid side converter. During this investigation, it is noteworthy that most studies have adopted the classical method indicated before for the extraction of harmonic currents. They also applied vector control using traditional PI controllers for both converters, without attempting to enhance the PI power flow controller response.

In this study, the neural-RIP (Real and Imaginary Instantaneous Powers) is used as the harmonic current identifier for the efficient and rapid harmonic current reference generation. A fuzzy PI controller is induced to improve the response of the powers flow to the stator. The simulation results have demonstrated the effectiveness and

the reliability of the suggested control in terms of harmonic compensation.

Modelling of DFIG

Fig.1 shows the diagram of the proposed filtering operation ensured by wind turbine based DFIG connected to the grid.

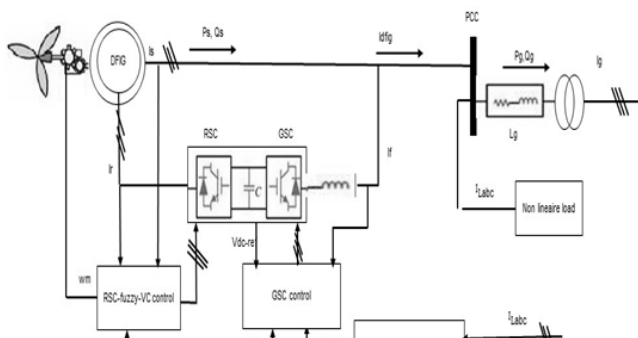


Fig.1 proposed diagram of SAF-DFIG operation

The doubly fed induction generator can be modelled in a synchronously rotating d-q reference frame, by the following equations

$$(1) \begin{cases} V_{ds} = R_s I_{ds} - \omega_s \varphi_{qs} + \frac{d\varphi_{ds}}{dt} \\ V_{qs} = R_s I_{qs} + \omega_s \varphi_{ds} + \frac{d\varphi_{qs}}{dt} \\ V_{dr} = R_r I_{dr} - (\omega_s - \omega_r) \varphi_{qr} + \frac{d\varphi_{dr}}{dt} \\ V_{qr} = R_r I_{qr} + (\omega_s - \omega_r) \varphi_{dr} + \frac{d\varphi_{qr}}{dt} \end{cases}$$

$$(2) \begin{cases} \varphi_{ds} = L_s I_{ds} + L_m I_{dr} \\ \varphi_{qs} = L_s I_{qs} + L_m I_{qr} \\ \varphi_{dr} = L_r I_{dr} + L_m I_{ds} \\ \varphi_{qr} = L_r I_{qr} + L_m I_{qs} \end{cases}$$

$$(3) C_{em} = \frac{3}{2} p \frac{M}{L_s} (\varphi_{qs} I_{dr} - \varphi_{ds} I_{qr})$$

$$(4) \begin{cases} P_s = \frac{3}{2} (V_{ds} I_{ds} - V_{qs} I_{qs}) \\ Q_s = \frac{3}{2} (V_{qs} I_{ds} - V_{ds} I_{qs}) \end{cases}$$

$$(5) \begin{cases} P_r = \frac{3}{2} (V_{dr} I_{dr} - V_{qr} I_{qr}) \\ Q_r = \frac{3}{2} (V_{qr} I_{dr} - V_{dr} I_{qr}) \end{cases}$$

here: V_{ds}, V_{qs} – stator voltages, V_{dr}, V_{qr} – rotor voltages, $\varphi_{s(d,q)}$ – stator flux, $\varphi_{r(d,q)}$ – rotor flux, C_{em} – electromagnetic torque, P_s, Q_s – active and reactive power of stator, P_r, Q_r – the active and reactive power of the rotor.

Vector control of the rotor side converter

The vector control is employed to ensure the control of the active and reactive powers of the stator independently. It can be further divided into the stator flux-oriented control (FOC) and the stator voltage-oriented control (VOC) by different orientations of the synchronous rotating frame. Fig.2 illustrates a synoptic diagram of the vector flux-oriented control of the RSC.

The Stator Flux orientation is based on the alignment of the stators flux with the rotating frame (d) axis. This may be represented through the expressions of the flux:

$$(6) \begin{cases} \varphi_{qs} = 0 \\ \frac{d\varphi_{qs}}{dt} = 0 \\ \varphi_{ds} = \varphi_s \end{cases}$$

substituting this condition in the mathematical equation of flux, currents, active and reactive power of stator the expressions of currents of the stator on dq axis are defined by the equation (7):

$$(7) \begin{cases} I_{qs} = I_{qr} * \frac{L_m}{L_s} \\ I_{ds} = \frac{\varphi_s}{L_s} - I_{dr} \frac{L_m}{L_s} \end{cases}$$

substituting (7) in (4) the expressions of active and reactive power of stator become

$$(8) P_s = -\frac{3}{2} \frac{L_m}{L_s} V I_{qr}$$

$$(9) Q_s = \frac{3}{2} \frac{L_m}{L_s} V (-I_{dr} + \frac{V_s}{L_m \omega_{sr}})$$

substituting (5) in the equations of the flux of the rotor and substituting the expression obtained in the mathematical expressions of the voltage of the rotor, the following expression is obtained

$$(10) \begin{cases} V_{dr} = R_r I_{dr} + L_r \sigma \frac{dI_{dr}}{dt} - \omega_{sr} L_r \sigma I_{qr} \\ V_{qr} = R_r I_{qr} + L_r \sigma \frac{dI_{qr}}{dt} + \omega_{sr} L_r \sigma I_{dr} + \omega_{sr} \frac{L_m * V_s}{L_s} \end{cases}$$

The Stator Flux orientation is based on the alignment of the stators flux with the rotating frame (d) axis. This may be represented through the expressions of the flux:

$$(6) \begin{cases} \varphi_{qs} = 0 \\ \frac{d\varphi_{qs}}{dt} = 0 \\ \varphi_{ds} = \varphi_s \end{cases}$$

substituting this condition in the mathematical equation of flux, currents, active and reactive power of stator the expressions of currents of the stator on dq axis are defined by the equation (7):

$$(7) \begin{cases} I_{qs} = I_{qr} * \frac{L_m}{L_s} \\ I_{ds} = \frac{\varphi_s}{L_s} - I_{dr} \frac{L_m}{L_s} \end{cases}$$

substituting (7) in (4) the expressions of active and reactive power of stator become

$$(8) P_s = -\frac{3}{2} \frac{L_m}{L_s} V I_{qr}$$

$$(9) Q_s = \frac{3}{2} \frac{L_m}{L_s} V (-I_{dr} + \frac{V_s}{L_m \omega_{sr}})$$

substituting (5) in the equations of the flux of the rotor and substituting the expression obtained in the mathematical expressions of the voltage of the rotor, the following expression is obtained

$$(10) \begin{cases} V_{dr} = R_r I_{dr} + L_r \sigma \frac{dI_{dr}}{dt} - \omega_{sr} L_r \sigma I_{qr} \\ V_{qr} = R_r I_{qr} + L_r \sigma \frac{dI_{qr}}{dt} + \omega_{sr} L_r \sigma I_{dr} + \omega_{sr} \frac{L_m * V_s}{L_s} \end{cases}$$

Fuzzy -PI controller for RSC control

The fuzzy control technique is predicated on some amount of human cognitive flexibility. It succeeds to provide an adequate performance without the requirement for the system's mathematical model, just by adding experts' knowledge contrary to traditional PI controller which depends on the parameters of the system and gives poor performance under any modification in the system's parameters [16-17].

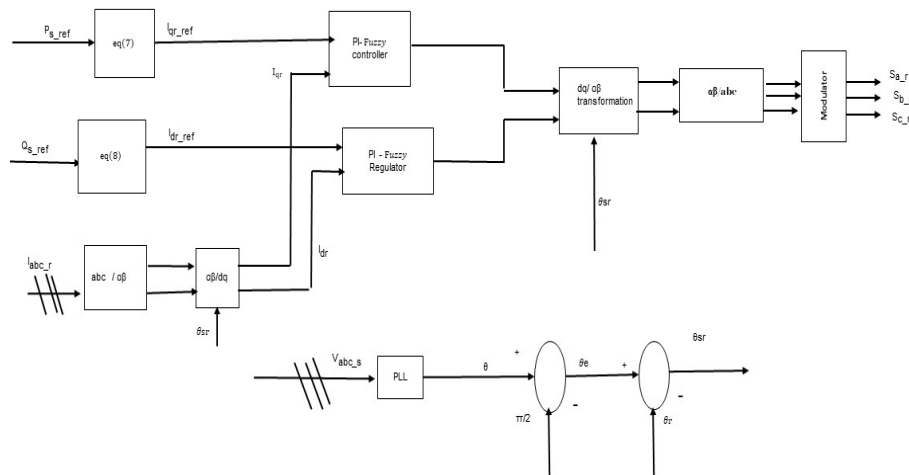


Fig.2 VC-FOC Synoptic Diagram OF RSC

The Mandani fuzzy inference method is extremely beneficial when applying fuzzy logic to system control. This mechanism is classified into three parts as shown in fig.3. The first is using input membership functions, the inputs are fuzzified, and then based on rule bases and inference system, outputs are produced and finally, the fuzzy outputs are defuzzified and applied to the system. The error and the error derivative rate are chosen as inputs in the case of designing this type of controller.

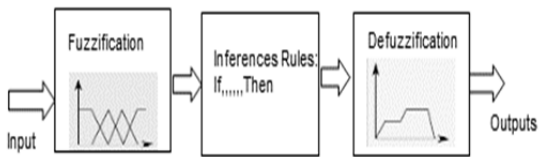


Fig.3 Block diagram of fuzzy control

The fuzzy controller designing for the active and reactive power used in this study is depicted in the block diagram of fig.4. The gains eG , ΔeG , and ΔuG are scaling factors (normalization). These parameters are modified till a suitable control is obtained. Indeed, the performance of the control depends on the value of those parameters.

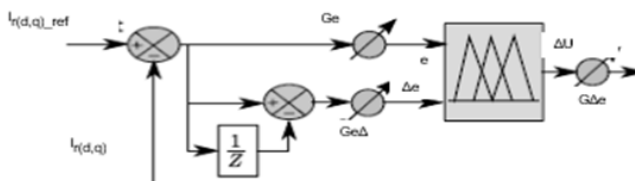


Fig.4 Design of a fuzzy controller

Table.1 Fuzzy rules

	E						
Δe	NB	NM	NS	Z	PS	PM	PB
NB	NB	NB	NB	NB	NB	NS	Z
NM	NB	NM	NM	NM	NS	Z	PS
NS	NB	NB	NM	NS	Z	PS	PM
Z	NB	NM	NS	Z	PS	PM	PB
PS	NM	NS	Z	PS	PM	PB	PB
PM	NS	Z	PS	PM	PB	PB	PB
PB	Z	PS	PM	PB	PB	PB	PB

It will be possible to define the membership functions using a fuzzy toolbox in MATLAB. Those membership functions are chosen to satisfy the best response results, here seven membership functions consist of five triangular functions and two Z-shaped membership functions (zmf)

are used on a universe of discourse normalized in the range [-1; 1]. The fuzzy rules are represented in Table 1, where the notations representation is as follows: *NB*: Negative Big, *NM*: Negative Medium, *NS*: Negative Small, *Z*: Zero, *PS*: Positive Small, *PM*: Positive Medium, and *PB*: Positive Big.

Vector control (VC) of the grid side converter GSC

The control of the grid side system is essential. The system cannot work correctly without it. Two main functions are ensured by the GSC, the first function is to keep the DC-bus voltage at the desired RSC level, whereas GSC currents must be sinusoidal and phased with the voltages for which the control system of the DFIG keeps the unity power factor condition and the second is to perform as shunt active filter for harmonic cancellation in the presence of non-linear load, in addition, to maintain a unity power factor on the grid side.

The control approach applied to the GSC is voltage vector control. The exposure of the dynamic modelling of the grid side converter is necessary to understand the behaviour of the system. It is possible to display the system configured in (*dq*) axis by a grid side converter, filter, and grid voltage in the following equation

$$(11) \quad \begin{cases} V_{df} = R_f I_{df} + V_{dg} + L_f \frac{dI_d}{dt} - \omega_s L_f I_{qg} \\ V_{qf} = R_f I_{qg} + L_f \frac{dI_q}{dt} + \omega_s L_f \sigma I_d + V_{qg} \end{cases}$$

Where: L_f – inductance filter R_f – resistance filter, V_{dg} , V_{qg} – grid voltages, V_{df} , V_{qf} – grid side converter voltages. Thus, the total active and reactive powers exchanged with the grid are expressed by the equation (12)

$$(12) \quad \begin{cases} P_g = \frac{3}{2} (V_{dg} I_{dg} + V_{qg} I_{qg}) \\ Q_g = \frac{3}{2} (V_{qg} I_{dg} - V_{dg} I_{qg}) \end{cases}$$

In order to perform the vector control technique, it's required to align the *d* axis of the rotating frame with the grid voltage space vector V_g as shown in Fig.5

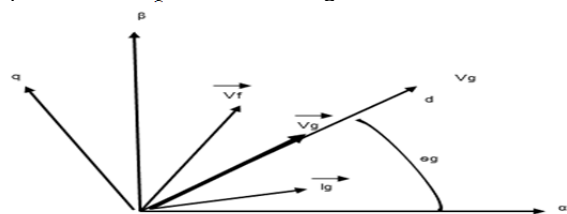


Fig.5 Alignment with d axis of the grid voltage space vector.

Sustaining the equations (13) in equation (11), results in equation (14)

$$(13) \quad \begin{cases} V_{qg} = 0 \\ V_{dg} = V_g \end{cases}$$

$$(14) \quad \begin{cases} V_{df} = R_f I_{dg} + V_{dg} + L_f \frac{dI_d}{dt} - \omega_s L_f I_{qg} \\ V_{qf} = R_f I_{qg} + L_f \frac{dI_q}{dt} + \omega_s L_f I_d \end{cases}$$

The total active and reactive powers are calculated by

$$(15) \quad \begin{cases} P_g = \frac{3}{2} V_{dg} I_{dg} \\ Q_g = -\frac{3}{2} V_{dg} I_{qg} \end{cases}$$

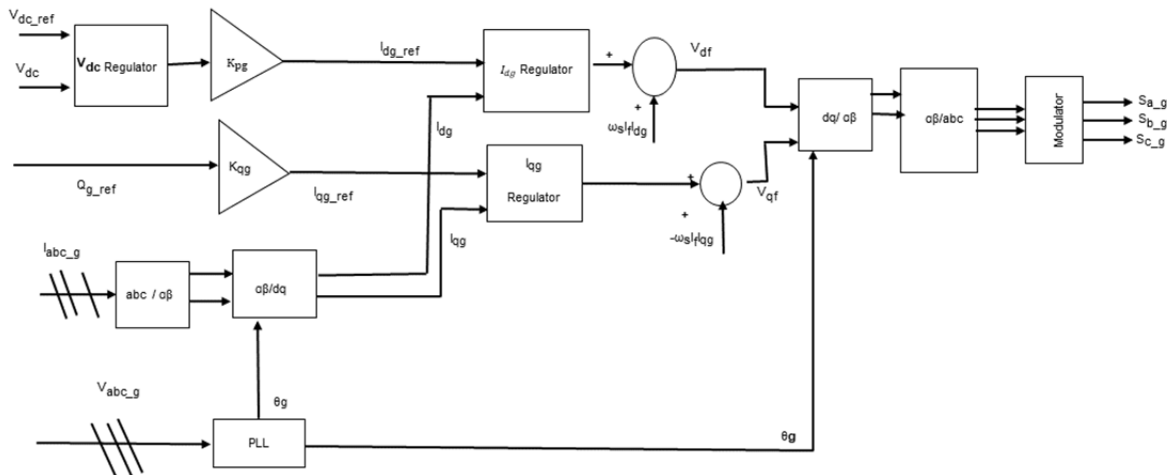


Fig.6 VC diagram of the GSC

It is noticed from the equation (15) that the value of the active power is controlled by the I_{dg} current while the I_{qg} current is responsible of the value of the reactive power as indicated in fig.6

For the DC-bus voltage it is necessary to give the dc bus voltage a model in order to define its PI parameters, so the model of dc bus voltage is given in the excessive equations from (16) to equation (18)

$$(16) \quad C_{dc} p V_{dc}^2 = -\frac{3}{2} V_{qg} I_{qg} \delta_{dc}$$

$$(17) \quad C_{dc} p V_{dc}^2 = \delta_{dc} = \left(K_{pdc} + \frac{K_{i dc}}{p} \right) (V_{dc}^{*2} - V_{dc}^2)$$

$$(18) \quad \frac{V_{dc}^2}{V_{dc}^{*2}} = \frac{\frac{1}{C_{dc}}}{p^2 + \frac{K_{pdc}}{C_{dc}} p + \frac{K_{i dc}}{C_{dc}}} (p K_{pdc} + K_{i dc})$$

Where: δ_{dc} – output of the q axis dc bus voltage controller $K_{pdc}, K_{i dc}$ –proportional and integral gains respectively, V_{dc}^* –the reference dc bus voltage

$$(19) \quad p^2 + \frac{K_{pdc}}{C_{dc}} p + \frac{K_{i dc}}{C_{dc}} = p^2 + \omega_{0dc} p \sqrt{2} + \omega_{0dc}^2$$

$$(20) \quad \begin{cases} K_{pdc} = C_{dc} \omega_{0dc} \sqrt{2} \\ K_{i dc} = C_{dc} \omega_{0dc}^2 \end{cases}$$

a proportional-integral controller is implemented for the grid currents I_{dg}, I_{qg} regulation, the parameters 's' value of the controller is calculated depending on the inner parameters of the grid side converter, the inductive filter and resistance filter.

The reference q- and d-axis GSC voltages can be expressed as:

$$(21) \quad \begin{cases} V_{df} = \delta_{df} \omega_s L_f I_{qg} \\ V_{qf} = \omega_s L_f I_{dg} + V_{qg} + \delta_{qf} \end{cases}$$

Where the controller outputs are defined as:

$$(22) \quad \begin{cases} R_f I_{qg} + L_f p I_{qg} = \delta_{df} = \left(K_{pq} + \frac{K_{i q}}{p} \right) (I_{qg}^{*2} - I_{qg}^2) \\ R_f I_{dg} + V_{dg} + L_f p I_{dg} = \delta_{qf} = \left(K_{pq} + \frac{K_{i q}}{p} \right) (I_d^{*2} - I_{dg}^2) \end{cases}$$

$$(23) \quad \frac{I_{qg}^2}{I_{qg}^{*2}} = \frac{\frac{1}{L_f}}{p^2 + \frac{R_f + K_{pq}}{L_f} p + \frac{K_{i q}}{L_f}} (p K_{pq} + K_{i q})$$

The current controller parameters are deduced from the following expression

$$(24) \quad p^2 + \frac{R_f + K_{pq}}{L_f} p + \frac{K_{i q}}{L_f} = p^2 + \omega_{0q} p \sqrt{2} + \omega_{0q}^2$$

$$(25) \quad \begin{cases} K_{pdc} = -R_f + L_f \omega_{0qf} \sqrt{2} \\ K_{i dc} = L_{dc} \omega_{0qf}^2 \end{cases}$$

The converters switching frequency f_{sw} is chosen:4 kHz. Given that the switching frequency, is 4 kHz, thus the bandwidth frequencies of the inner loop and outer loop are given by the following expressions:

$$(26) \quad \begin{cases} K_{pdc} = \omega_{0qf} = 2 * \pi * f_{sw} / 10 \\ \omega_{0dc} = \omega_{0qf} / 10 \end{cases}$$

Active power filter in the GSC

Non linear loads are the main responsible of the harmonic currents emission in the electrical system. Those harmonic currents lead to many undesirable effects on the electrical elements as well as their function and performance. Shunt active filter comes as a solution to resolve this problem. Through this study, the grid side converter is employed as a shunt active filter due to the similar configuration between the two of them. By modifying the control structure with the adding of the extracted current harmonics I_{dh} and I_{qh} to the reference currents in inner current loop control as shown in fig.7.

So, the new reference current I_{dg}^*, I_{qg}^* can be expressed by the equation (27)

$$(27) \quad \begin{cases} I_{dg}^* = I_{dg_ref} + I_{dh} \\ I_{qg}^* = I_{qg_ref} + I_{qh} \end{cases}$$

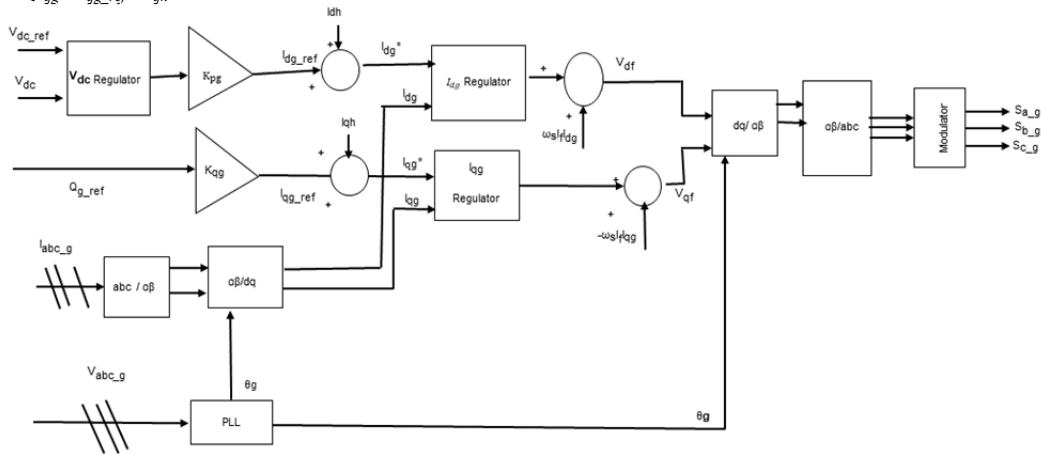


Fig.7 Diagram of GSC system control

Neural-RIP (Real and Imaginary Instantaneous Powers) Method

A large number of fields have seen the use of the neural network to tackle technological challenges. Power system is one of those fields, particularly for harmonic detection in alternating current supply systems. [19] Neural-RIP is a technique used for harmonic identification. It involves the use of two ADALINE networks to define harmonics instead of two low-pass filters which are utilized in the classical RIP method defined in the following equation

$$(28) \quad \begin{bmatrix} v_{ga} \\ v_{gb} \\ v_{gc} \end{bmatrix} = \sqrt{\frac{2}{3}} \begin{bmatrix} 1 & -1/2 & -1/2 \\ 0 & \sqrt{3}/2 & -\sqrt{3}/2 \end{bmatrix} \begin{bmatrix} v_{ga} \\ v_{gb} \\ v_{gc} \end{bmatrix}$$

$$(29) \quad \begin{bmatrix} i_{ga} \\ i_{gb} \\ i_{gc} \end{bmatrix} = \sqrt{\frac{2}{3}} \begin{bmatrix} 1 & -1/2 & -1/2 \\ 0 & \sqrt{3}/2 & -\sqrt{3}/2 \end{bmatrix} \begin{bmatrix} i_{ia} \\ i_{ib} \\ i_{ic} \end{bmatrix}$$

The instantaneous active and reactive power are obtained by

$$(30) \quad \begin{bmatrix} p \\ q \end{bmatrix} = \begin{bmatrix} v_{ga} & v_{gb} \\ -v_{gb} & v_{ga} \end{bmatrix} \begin{bmatrix} i_{ia} \\ i_{ib} \end{bmatrix}$$

Each one of the powers (active P and reactive Q) contain a continuous part and an alternative part, which lead to the next expression:

$$(31) \quad \begin{bmatrix} p \\ q \end{bmatrix} = \begin{bmatrix} \bar{p} + \tilde{p} \\ \bar{q} + \tilde{q} \end{bmatrix}$$

where: \bar{p} , \bar{q} -continuous components related to the fundamental components of P and Q. \tilde{p} , \tilde{q} -alternate components relating to the harmonics.

The current references are then given by:

$$(32) \quad \begin{bmatrix} i_a \\ i_b \end{bmatrix} = \frac{1}{v_{ga}^2 + v_{gb}^2} \begin{bmatrix} v_{ga} & -v_{gb} \\ v_{gb} & v_{ga} \end{bmatrix} \begin{bmatrix} p \\ q \end{bmatrix}$$

After finding the α - β reference current, the compensating current for each phase can be derived by using the inverse Clarke transformations as shown in the following equation:

where: I_{dh} , I_{qh} —harmonic current of non-linear load, I_{dg} , I_{qg} —a currents of the grid side converter.

The method used to identify harmonic currents is neural-RIP which will be explained in details in the next section.

$$(33) \quad \begin{bmatrix} i_{aref} \\ i_{bref} \\ i_{cref} \end{bmatrix} = \sqrt{\frac{2}{3}} \begin{bmatrix} 1 & 0 \\ -1/2 & \sqrt{3}/2 \\ -1/2 & -\sqrt{3}/2 \end{bmatrix} \begin{bmatrix} i_a \\ i_b \end{bmatrix}$$

The two ADALINE networks utilized to identify the harmonic current are displayed in Fig .8

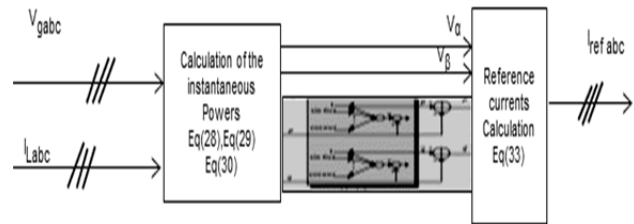


Fig.8 RIP-ADALINE structure for harmonic current extraction

The identification and the separation of alternate components \tilde{p} , \tilde{q} from continuous components \bar{p} , \bar{q} are ensured by the two Adaline network similarly to the function of the low pass filter.

The signal is a summation of many sinusoidal components including the fundamental wave and harmonic waves where every component characterizes by its magnitude and its frequency thus for each sample k and sampling period t_s the signal can be presented by the following equation

$$(34) \quad S_i(k) = \sum_{n=1,2,\dots}^N [W_{an} \sin(nk\omega t_s) - W_{bn} \cos(nk\omega t_s)]$$

here: W_{an} , W_{bn} —the magnitude of the sine and cosine, N —maximum harmonic order to n .

Taking that the signal S_i could be a current or voltage Using a frequency analysis, the expression (31) of the instantaneous powers can be writing as follow

$$(35) \quad p = p_1 \cos(\alpha) + p_3 \cos(6\omega t - 5\alpha) - p_7 \cos(6\omega t - 7\alpha) - \dots$$

$$(36) \quad q = -q_1 \sin(\alpha) - q_3 \sin(6\omega t - 5\alpha) - q_7 \sin(6\omega t - 7\alpha) + \dots$$

Where: $p \cos \alpha, -q \sin \alpha$ –the continuous parts (\bar{p}, \bar{q}), the rest of terms represent the alternative parts (\tilde{p}, \tilde{q}).

To estimate active and reactive powers, two Adalare are established, where the inputs are sinusoidal functions that represent each harmonic order in the mathematical developments expressed in equations (34) and (35).

In the general case, Fourier's analysis may represent the real and imagined instantaneous power as follow:

$$(37) \quad F(t) = A_0 + \sum_{n=1,2,\dots}^N A_{n1} \cos(n\omega t - (n-1)\alpha) + A_{n2} \cos(n\omega t + (n-1)\alpha) + B_{n1} \sin(n\omega t - (n-1)\alpha) + B_{n2} \sin(n\omega t + (n-1)\alpha)$$

Where: A_0 –the continuous component, A_{n1}, A_{n2}, B_{n1} – the sinus and cosine amplitudes.

The rearranging of the equation (37) in vector form gives the following expression

$$(38) \quad \overline{F(t)} = \overline{W^T} \overline{X(t)}$$

$$(39) \quad \overline{W^T} = [A_0 \ A_{11} \ A_{12} \ B_{11} \ B_{12} \ \dots \ A_{n1} \ A_{n2} \ B_{n1} \ B_{n2}]$$

Where: $\overline{W^T}$ –the weight matrix, $\overline{X(t)}$ –cosine and sine vector. Thus, the neuron demonstrated in the fig. 8 is implemented depending on the equation (38) where the inputs are the cosine and sin components, the weights are the amplitudes of the inputs.

The signal of the active and reactive powers and its components are identified and estimated, the neural weights are updated using the Learning algorithm (Widrow-Holf) expressed by the following equation

$$(40) \quad \overline{W(k+1)} = \overline{W(k)} + \mu e(k) \overline{X(k)}$$

Where: $W(k)$ – the neural weight at (k) time, $e(k)$ –the error between the estimated signal of the active and reactive powers and the real ones at (k) time, $X(k)$ –the input vector at (k) time, μ –the learning coefficient

Results and discussion

The proposed control strategy was tested through the simulation of the system indicated in fig.1 using MATLAB /Simulink/simpowersys environment. The parameters of the DFIG used in the simulation are shown in the table.2

Table.2 Parameters of the DFIG

Magnitudes and parameters	Value with unit
Rated power P_s	$P_s=1.5$ Mw
Source voltage/ frequency f_s	$V_s=690$ V/ $F_s=50$ Hz
Stator resistance / Rotor resistance	$R_s=2.6$ m Ω / $R_r=2.9$ m Ω
stator inductance / rotor inductance / Mutual inductance	$L_s=2.56$ mH / $L_r=2.56$ mH/ $L_m=2.5e-3$ mH
Number of poles	2
Switching frequency	$F_{sw}=4$ KHz

The system consists of wind turbine based DFIG connected to the grid utility, both sources are feeding a nonlinear load that contains a rectifier and R; L load and their parameters are indicated in table.3, the non-linear load effects the shape of current at the point of common coupling which leads automatically to the degradation of the power quality due to harmonics presence in the circuits. Two cases are studied: before and after the filtering operation.

Table.3 Parameters of non lineaire load

Magnitudes and parameters of non lineaire load	Value with unit
Input inductance / Input resistance R	0.56 mH/1 Ω
Load resistance	8 Ω

1) Before the filtering operation

The results of the simulation without the inclusion of the filtering process are illustrated in fig. 9 to fig.14

In this case the DFIG function in the traditional mode as a provider of powers. Fig.9 presents the response of the active and reactive powers of the stator and fig. 10 presents the currents of the rotor, it's obvious that the measured value of the current of the rotor in dq axis i_{dr} and i_{qr} follow the references i_{dr} and i_{qr} controlling the power P_s and Q_s respectively.

The waveforms of the grid voltage, generator, non-linear load and electric grid currents are obtained for the system and shown in fig.12.

Fig.13 illustrates the current waveform at the PCC and its spectrum analysis. The grid current is distorted and shows a THD equal to 26.78% at 150 rad/s. This current distortion is due to the presence of the harmonic components of 5th, 7th, 11th and 13th orders. The harmonics in the electrical grid can cause a distorted voltage to other consumers connected to the PCC of the grid current.

The non-linear load current and its harmonic spectrum are shown in fig.14. The waveform of the load current is distorted and its THD ratio is equal to 26.90%, which indicates a serious harmonic content that affects the grid source currents by a high harmonic level pollution

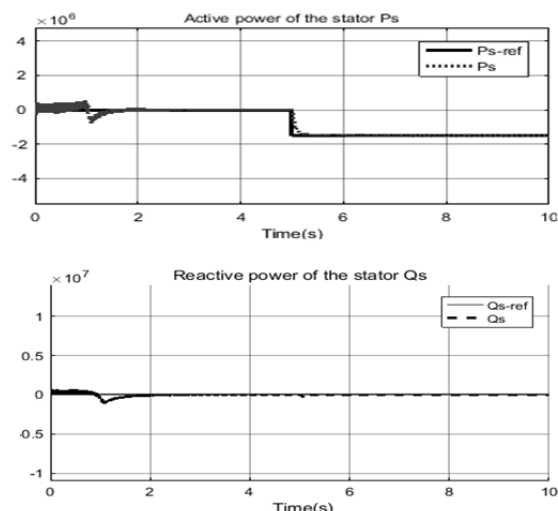


Fig 9 Response of the reactive and active powers of the stator

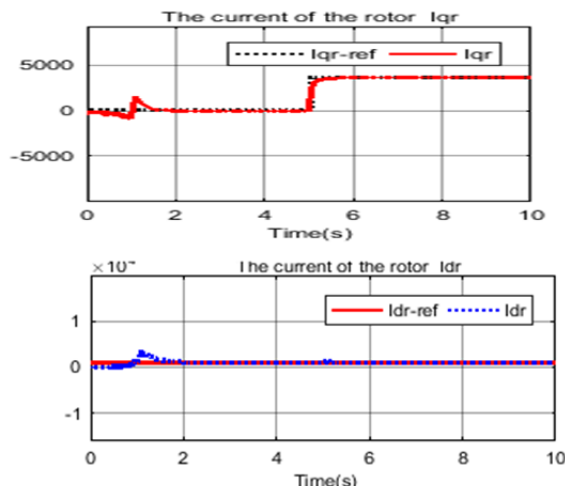


Fig.10 Response of the current I_{qr} and I_{dr}

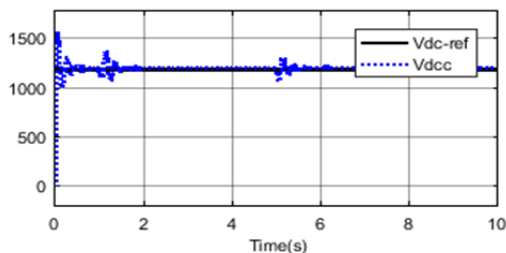


Fig 11 Response of control loop of the dc link voltage.

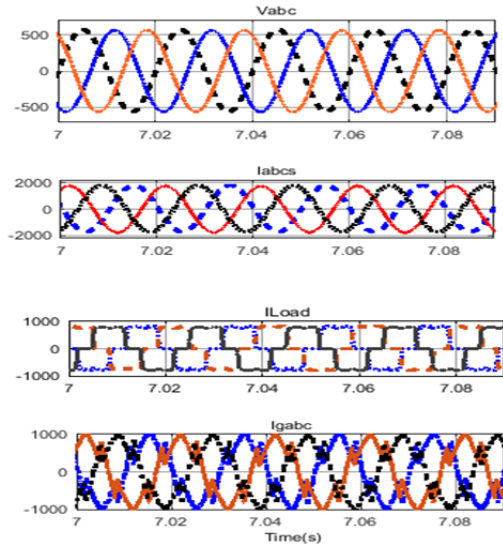


Fig 12 Waveforms of the voltage of DFIG, stator currents, non-linear load currents, and grid currents

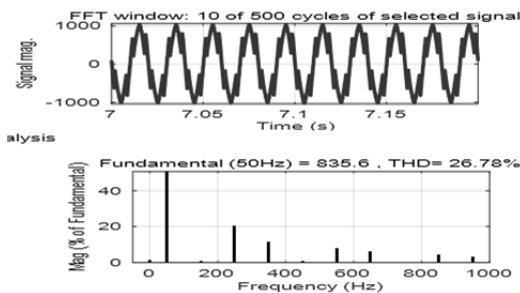


Fig 13 Spectrum analysis of the grid current

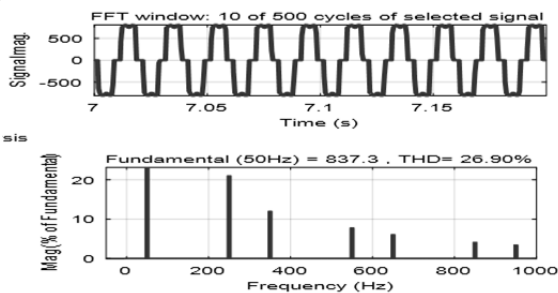


Fig.14. Spectrum analysis of the load current

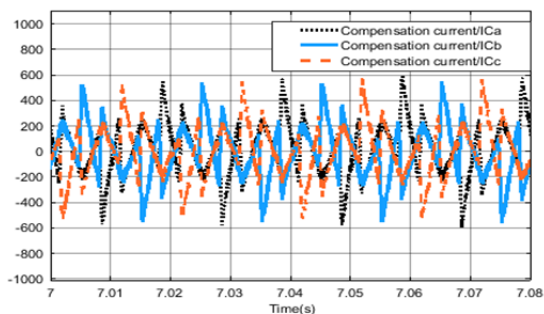


Fig.15 The injected compensated current identified by neural RIIP

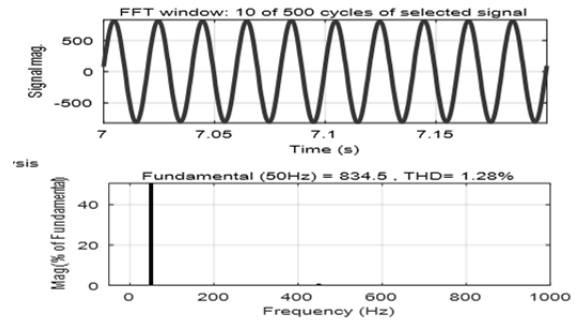


Fig.16 The waveform of the grid current after the active filtering

2) After the performing of the filtering operation at the level of the GSC

In this case the grid side converter ensures the active filtering in addition to its traditional function, the GSC works as shunt active filter providing the required compensated currents, the neural-RIP technique is used to identify harmonics current, the performance of the DFIG as shunt active filter is simulated and the results are carried out in fig.16.

The currents of the rotor and the active and reactive powers give the same response as in the first case due to the similar control system applied on the rotor side converter in both cases.

Fig.15 indicates the compensated current generated by the RIP- ADALINE technique

Fig .16 shows the grid current waveform after the applying to the filtering approach explained previously. It's noticed through the response of the waveform that the grid current return to its sinusoidal form recording a THD ratio equal to 1.28%. The value of THD recorded during this study is lower value than those recorded in [13,16] which reflect the effectiveness of the neural RIP in the harmonic precision and their separation. The obtained THD ratio after the proposed filtering process that depends on the grid side converter and the technique used to identify harmonics in the electrical system has proved the effectiveness and the reliability of the method used. This technique gives better outcomes than the conventional method due to the precision in obtaining the continuous components.

Conclusion

This study examines the use of the grid side converter of the wind turbine-based DFIG as a shunt active filter to improve the power quality in the grid-connected to the wind power plant.

The control vector strategy was applied to control the converters of the DFIG. A fuzzy-PI controller was designed to control the active and reactive power flowing in the rotor side converter due to its benefits and characteristics like fast response and robustness. To identify harmonics in the electrical system a neural RIP approach was explained and implemented. This technique characterizes by its precision in obtaining the continuous components compared to the classical methods.

The compensating currents calculated by this technique are added to the current reference in the inner control loop of the grid side converter. With the increased use of the non-linear load, the wind power plant must provide other services like the filtering operation to improve the power quality in the electrical systems. The application of shunt active filter in the grid side converter had shown its effectiveness in improving the power quality of the grid current through the lower value of the THD obtained, thus it was reduced from 26.78 % to 1.28%.

Authors

Khelifa Siham, ICEPS laboratory, PhD student Science faculty, Electrical Engineering Department, Djillali Liabes of Sidi Bel Abbas 22000, Algeria Email: sihamsiam71@gmail.com

REFERENCES

- [1] Kaloi, Ghulam Sarwar, Wang, Jie, et Baloch, Mazhar Hussain. Active and reactive power control of the doubly fed induction generator based on wind energy conversion system. *Energy Reports*, 2016, vol. 2, p. 194-200.
- [2] Om Prakash Bharti, R. K. Saket, S. K. Nagar, 'Controller Design of DFIG Based Wind Turbine by Using Evolutionary Soft Computational Techniques', *Engineering, Technology & Applied Science Research* Vol. 7, No. 3, 2017, 1732-1736
- [3] Tapia, Arantxa, et al. "Modeling and control of a wind turbine driven doubly fed induction generator." *IEEE Transactions on energy conversion* 18.2 (2003): 194-204.
- [4] El Kachani, Abderrahmane, Laachir, Anass Ait, Niaaniaa, Abdelhamid, et al. DFIG-Based Wind Turbine with Shunt Active Power Filter Controlled by Double Nonlinear Predictive Controller. *International Journal of Energy and Power Engineering*, 2017, vol. 9, no 12, p. 1515-1522.
- [5] Reis, Alex, Moura, Leandro P., et De Oliveira, José C. Mitigation of harmonic current produced by wind turbine throughout converter switching control. In : *2016 17th International Conference on Harmonics and Quality of Power (ICHQP)*. IEEE, 2016. p. 255-260.
- [6] Hoseinpour, Alireza, S. Masoud Barakati, and Reza Ghazi. Harmonic reduction in wind turbine generators using a Shunt Active Filter based on the proposed modulation technique. *International Journal of Electrical Power & Energy Systems*, 2012, vol. 43, no 1, p. 1401-1412
- [7] Balaji, R., and B. Mohamed Faizal. Design of Shunt Active Filters based on Phase Locked Loop and PI Controller. *International Journal of Soft Computing and Engineering (IJSCE)*, 2014, vol. 4, p. 60-63.
- [8] Zahim, S. M. et Erlich, I. Control of DFIG based Wind Turbine Converter using Continuous and Discontinuous PWM: A Comparative Study. *IFAC Proceedings Volumes*, 2012, vol. 45, no 21, p. 542-547.
- [9] Kesraoui, M., et al. Using a DFIG based wind turbine for grid current harmonics filtering. *Energy Conversion and Management*, 2014, vol. 78, p. 968-975.
- [10] Nosrabadi, Seyyed Mostafa et Gholipour, Eskandar. Power system harmonic reduction and voltage control using DFIG converters as an active filter. *Turkish Journal of Electrical Engineering & Computer Sciences*, 2016, vol. 24, no 4, p. 3105-3122.
- [11] Kairus, Djilali, et al. Variable structure control of DFIG for wind power generation and harmonic current mitigation. *Advances in Electrical and Computer Engineering*, 2010, vol. 10, no 4, p. 167-174.
- [12] Mishra, Anirban, and Kalyan Chatterjee. Power Quality Enhancement of DFIG based Wind Turbine by Active Filter Implementation. In : *2019 International Conference on Ubiquitous and Emerging Concepts on Sensors and Transducers (UEMCOS)*. IEEE, 2019. p. 1-6
- [13] Ali, Hazem Hassan, and Gaber ElSaady. Grid Side Converter Based Shunt Active Power Filter of Variable Speed Doubly Fed Induction Generator Driven by Wind Turbine. *Journal of Electrical Engineering*, 2017, vol. 17, no 4, p. 12-12
- [14] Naidu, NK Swami, and Bhim Singh. Doubly fed induction generator for wind energy conversion systems with integrated active filter capabilities. *IEEE transactions on industrial informatics*, 2015, vol. 11, no 4, p. 923-933.
- [15] BabyPriya, B., and A. Chilambuchelvan. Modelling and analysis of DFIG wind turbine harmonics generated in grids. *International Journal of Engineering and Technology*, 2010, vol. 2, no 3, p. 185-189.
- [16] Souza, Ramon R., et al. A proposal for a wind system equipped with a doubly fed induction generator using the conservative power theory for active filtering of harmonics currents. *Electric Power Systems Research*, 2018, vol. 164, p. 167-177.
- [17] Karimi-Davijani, H., et al. Fuzzy logic control of doubly fed induction generator wind turbine. *World Applied Sciences Journal*, 2009, vol. 6, no 4, p. 499-508.
- [18] Azzaoui, Marouane El, and Hassane Mahmoudi. Fuzzy-PI control of a doubly fed induction generator-based wind power system. *International Journal of Automation and Control*, 2017, vol. 11, no 1, p. 54-66.
- [19] Abdeslam, Djaffar Ould, et al. A unified artificial neural network architecture for active power filters. *IEEE transactions on industrial electronics*, 2007, vol. 54, no 1, p. 61-76.